ELSEVIER

Journal of Nuclear Materials 289 (2001) 57–70

journal of nuclear materials

www.elsevier.nl/locate/jnucmat

Section 2. Fundamental radiation effects in ceramics

Molecular dynamics simulation of irradiation-induced amorphization of cubic silicon carbide

L. Malerba *,[1], J.M. Perlado

Instituto de Fusión Nuclear (DENIM), Universidad Politécnica de Madrid, C/ José Gutiérrez Abascal, 2, Madrid 28006, Spain

Abstract

It has long been observed that a crystalline-to-amorphous (c-a) transition occurs in silicon carbide (SiC) irradiated at low temperature. However, the microscopic mechanisms leading to the transition are not well understood. We report in this paper a molecular dynamics (MD) simulation of low-energy (100 eV) recoil accumulation at cryogenic temperature (20 K), up to ≈1 dpa, in which the irradiated computational sample becomes amorphous and is subsequently annealed at high temperature (2320 K). The simulation suggests that, at least for low-mass impinging particles, provided that no direct impact amorphization (DIA) takes place, the driving force for the c-a transition in this material is the accumulation of Frenkel pairs up to a critical concentration ($\approx 1.9 \times 10^{22}$ cm^{-3}). The role of antisites in the process is negligible. In fact, antisite formation during the annealing could be the bottleneck for complete recovery. A simple and intuitive analytical model based on the concepts of recombination barriers and interstitial migration is also proposed, to describe the temperature dependence of the critical dose for amorphization. © 2001 Published by Elsevier Science B.V.

PACS: 61.43.Bn; 61.43.Dq; 61.82.−d; 61.80.−x

1. Introduction

Silicon carbide (SiC), a low-activation, low-Z, high-temperature-resistant material, has long been considered for performing structural and protective functions in the first wall and blanket of future nuclear fusion reactors [1], both magnetic [2–4] and inertial [5–7], particularly in the form of SiC-fibre/SiC-matrix composite [8].

Since the early seventies, and especially in the last decade, an impressive quantity of work has been devoted to the study of ion- [9–35], electron- [36–40] and neutron- [41,42] irradiation-induced amorphization in SiC, and in ceramics in general [36,38,43–49]. What prompted this proliferation of papers was mainly the possible use of SiC as a semiconductor for the fabrication of high-temperature-resistant electronic devices [10–17,20,27,31–35,43–46,48,49,51]. Thanks to this large amount of studies, it is now well established that SiC can only be rendered amorphous by irradiation *below* a certain threshold temperature, which in no case has been reported to exceed 500 K [21,28,36–39,42,50–54]. Therefore, there appears to be no concern regarding the risk that SiC may amorphize in the range of operating temperatures typical of SiC-based nuclear fusion reactors (≈1000°C). However, the study of the mechanisms leading this material to disordering and amorphization by irradiation represents an important challenging issue also from the standpoint of nuclear applications, in order to achieve a deeper insight into the physics of SiC response to irradiation [9,18,19,21–26,28–30,38,41,42,47,50,52–54]. In particular, in spite of all the investigations, the microscopic mechanism responsible for the crystalline-to-amorphous (c-a) transition in SiC has not been identified yet with certainty. The possible causes debated, by comparison with other materials (monatomic semiconductors, intermetallic alloys), are direct impact amorphization (DIA) [55,56] and accumulation of damage up to a critical defect concentration (CDC)

* Corresponding author. Tel.: +34-91 3363108; fax: +34-91 3363002.

E-mail address: lmalerba@sckeen.be (L. Malerba).

[1] Current address: SCK-CEN, Boeretang 200, 2400 Mol, Belgium. Fax: +32-14 321216.

0022-3115/01/$ - see front matter © 2001 Published by Elsevier Science B.V.
PII: S0022-3115(00)00684-X

[57–60]. The fact that SiC is amorphized by electron irradiation [36–40] strongly supports the second possibility – as will be discussed – but it is still unclear whether the type of defects triggering the transformation are antisites [37,39,61–63] or Frenkel pairs [64–66], or both [67]. Moreover, for high-mass impinging ions DIA cannot be completely ruled out [68].

In this paper we report the results of a molecular dynamics (MD) simulation of the amorphization of cubic SiC induced by low-energy (100 eV) recoils and discuss them on the basis of past experimental and theoretical work. It turns out that the simulation compares well with experimental evidence, can be extended to the case of higher-energy recoils and supports theoretical models based on the accumulation of Frenkel pairs. As it is, the reported existence of energy barriers to Frenkel pair recombination in SiC [69–72] makes it feasible to store metastable point defects up to the required concentration. Based on this idea, a simple analytical model is proposed. By using it to interpolate experimental data points it is suggested that, in addition to recombination barriers, interstitial migration plays a role in determining the temperature dependence of the critical dose for amorphization.

2. Experimental and theoretical background

Since irradiation-induced amorphization was reported by Bloch in nuclear materials [73], this phenomenon has been observed and investigated in a variety of solids: metals, semiconductors and ceramics [36,62,74]. Historically, intermetallic alloys and monatomic semiconductors were most intensively studied [62,74]. In all cases, the experimentally observed behaviour is very similar and, though in this paper reference is made mostly to SiC studies, most phenomenological details can be generalised to other materials [62]. In particular, there always exists a critical radiation dose for amorphization, D_c, above which the transition takes place in a layer located at the depth of highest radiation-damage density [11–30,43–47]. Until this critical level of irradiation is reached, the process leading to the formation of the amorphous layer is normally heterogeneous (coalescence of amorphous islands) [10,19,21, 27,31,39–42,50] and the buildup of the amorphous fraction versus accumulated dose, as measured by Rutherford Backscattering-Channelling (RBS-C) [11–30,43–47,50–54] or other experimental techniques [9, 10,31–42,48,49], can generally be approximated by a sigmoidal ('S') curve [16,17,19,21,30,35,43,45,48,49], though in some cases the growth appears practically linear [11–13,32–34,75]. The critical dose for amorphization strongly depends on the irradiation temperature, to such an extent that, whereas at cryogenic level it may be reasonably easy to achieve irradiation-induced amorphization, there exists a critical value, T_c, above which it ceases to be possible to render the material amorphous, however high the dose. Qualitatively, the function $D_c(T)$ can be described by the curve in Fig. 1 [21,28,52,56,62]. This temperature dependence suggests that the c-a transition is only possible as long as the recovery rate by diffusion, or by other mechanisms of defect rearrangements, is slow in comparison with the damage-production rate, that is, a competition between opposite mechanisms, one of them thermally activated, is involved [56,57,60,62,65–67]. The actual value of the critical dose and temperature clearly depends on the material and in some cases it turns out to be impossible to produce amorphization, at any dose and temperature. Many empirical and theoretical criteria have been proposed to establish *a priori* the amorphizability of a material [36,63,76], but none of them have proved to be universally applicable. The critical dose and temperature also depend on the type and energy of the radiation used (stopping power) [26,48,49,51,52], as well as on the dose-rate, though the latter dependence appears to be very feeble and there is hardly any systematic study on this issue [25].

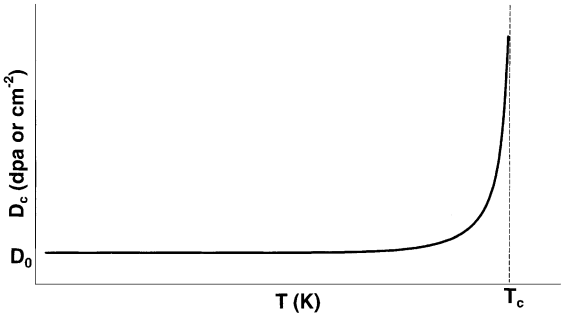

Fig. 1. Typical qualitative aspect of the curve representing the variation of the critical dose for amorphization, D_c, as a function of irradiation temperature for any amorphizable material. Note the vertical asymptote in correspondence of the critical temperature T_c.

In view of elaborating a theory capable of accounting for the phenomenology just described, it is important to distinguish between materials that are electron-irradiation amorphizable and materials that are not. Most intermetallics and ceramics belong to the former group; pure semiconductors (Si, Ge) belong to the latter [62]. In ion-irradiated pure semiconductors there is clear experimental evidence of DIA, that is, amorphous pockets are formed within single displacement cascades [55], as shown also in recent MD simulations for Si [77]. However, DIA alone cannot explain the buildup of an amorphous layer in a material: it has been long demonstrated, by using ever more refined theoretical models, that the sigmoidal buildup is a macroscopic manifestation of the necessity of some kind of damage overlap-

ping, in order to induce the c-a transition [59,60,78,79]. Nonetheless, DIA is considered as one of the fundamental mechanisms for amorphous-island nucleation and growth in pure silicon [56,79,80]. On the other hand, it is not clear what role DIA may play, if any, in materials that can be rendered amorphous by electron irradiation. As it is, this type of radiation is incapable of generating displacement cascades, so that the only possible mechanism leading to amorphous-layer formation by electron bombardment is the accumulation of a CDC, above which the system finds energetically more favourable collapsing into the amorphous state than persevering in a highly damaged crystalline state [57,58,62]. Clearly, when the material is heavy-ion implanted the existence of a component of DIA cannot be excluded [78]. Nevertheless, in the case of SiC many indications suggest that DIA should be ruled out, in most cases, even when the c-a transformation is induced by ion irradiation (except, perhaps, for very-high-mass ions [68]): (1) According to McHargue, the formation of amorphous pockets within displacement cascades below the critical dose is excluded by the observation of an increased hardness in subcritically ion-irradiated SiC [75]; (2) Musumeci et al. observe that the critical energy density for amorphization in SiC scarcely depends on the cascade energy, as opposite to Si [32]; (3) No electron microscopy detection of disordered zones of the size of a typical displacement cascade in subcritically ion-irradiated SiC has ever been reported, as opposite to Si or Ge [19,21,39,40,52]; (4) Recent MD simulations show that the cascade thermal spike is not capable of producing phase-change to liquid in SiC, thereby preventing the formation of amorphous pockets at the end of the cascade [70,81].

The theoretical models proposed in the literature to explain the process of irradiation-induced amorphization (mainly for intermetallics), claiming that the basic mechanism is the buildup of a CDC, can be reduced to two categories: one suggesting that the accumulation of vacancies and/or interstitials is the transformation driving force [64–66]; the other more prone to ascribe the effect to the accumulation of disorder (antisites) [61,62]. The main problem with models based on the former assumption is that they need to propose credible mechanisms preventing Frenkel pair recombination, a task that turns out to be particularly difficult in the case of metals, where interstitial diffusion is non-negligible even at very low temperature. In spite of these difficulties, the rate-equation model by Pedraza [65,66] seems self-consistent and enables one to interpolate correctly data points obtained by electron-irradiation experiments. On the other hand, the qualitative model proposed by Luzzi et al. [61,62], that makes antisites responsible for the c-a transition, is supported by the experimental observation of a high degree of disorder in intermetallics (long-range order parameter equal to 0.3 [61]) right before the transformation and *only* in the temperature range of amorphizability. Finally, Motta and Olander proposed that both defects should play a role in the phenomenon [67].

For ceramics in general, and for SiC in particular, no specific, rigorous model has been proposed. Nonetheless, the experimental data points describing the function $D_c(T)$ have been successfully interpolated by Weber [21,28,52] using the following expression, actually derived from the implicit assumption of DIA [82]:

$$D_c(T) = \frac{D_0}{[1 - C\exp(-E_a/nk_BT)]^m}, \tag{1}$$

where D_0 is the experimental value encountered for the critical dose at 0 K, C a dose-rate- and radiation-type-depending constant and E_a is a generic activation energy (k_B is the Boltzmann constant). By tuning the value of the integer exponents m and n, Weber's ($m = n = 1$) [82], Morehead and Crowder's ($m = n = 2$) [56] and Dennis and Hale's ($m = 2,\ n = 1$) [60] models can be obtained. The problem with expression (1) is that, whatever the choice of the exponents, the 'best-fit' activation energy is too low to be physically meaningful in a ceramic material like SiC ($\leqslant 0.3$ eV) [52], as pointed out by Snead and Zinkle [50]. Moreover, it is substantially an empirical formula, lacking any clear relationship with definite microscopic mechanisms. Snead and Zinkle made an attempt to adapt for SiC the model by Motta and Olander [67], that is, they adopted the following formula to interpolate their experimental data [50]:

$$D_c(T) = D_0 + \frac{A}{\sqrt{\Phi}}\exp\left(-\frac{E_m^i}{2k_BT}\right), \tag{2}$$

where E_m^i is the interstitial migration energy, A an adjustable constant and Φ is the dose-rate (in dpa/s). The serious shortcoming of expression (2) is that, though well adjustable to the experimental data in the intermediate temperature range, it does not predict the existence of a vertical asymptote, in correspondence with the critical temperature T_c.

3. Computational details

All simulations herein reported were carried out with the MD parallel program MDCASK, a code optimised for studying the interaction of high-energy ions with crystals [83]. The interatomic forces are described, in the case of SiC, using the Tersoff potential [84,85], merged with a binary ab initio repulsive potential, to adequately treat the atomic collisions in the short-distance range (>0.5 Å)[86,87]. The Tersoff potential has been long demonstrated to allow the performance of reliable MD simulations of the behaviour of SiC in a variety of conditions and situations [88–90], including the

amorphous state [91–93]. The MDCASK code is implemented in the Cray-T3E massively parallel supercomputer of the CIEMAT (Madrid, Spain), which can make available up to 32 processors for a single computational task. The parallel implementation is based on the PVM message-passing library.

For the simulation, a $6a_0 \times 6a_0 \times 6a_0$ ($a_0 = 4.36$ Å) constant volume box was used, containing a fixed number of 1728 atoms. Such a small box-size was selected in view of covering time-spans as long as 25 ns in an acceptable amount of CPU time. A three-step procedure was followed: (1) a computational amorphous–SiC sample, to be used as a reference, was generated by heat treatment; (2) by accumulating low-energy (100 eV) displacement cascades (whose size could be easily contained in the small simulation box chosen) at 20 K, the reproduction of the reference amorphous topology and energetics was attempted; (3) the computational irradiation-amorphized sample thereby obtained was heated and then isothermally annealed at 2320 K for 25 ns; the reference amorphous sample was also annealed in the same way. The temperature was controlled by using the velocity rescaling method, applied to the sole outer box-shell when the recoils were introduced. The choice of accumulating damage at very low temperature was dictated by the necessity of reaching the critical dose for amorphization at the lowest computational cost. For analogous reasons, the recovery processes were accelerated by annealing the material at very high temperature.

To generate the reference amorphous sample, a system with crystalline initial conditions was heated up to 13 000 K, maintained at that temperature for 40 ps and then relatively slowly cooled down to 300 K in two stages ($13\,000 \rightarrow 5000$ K, $5000 \rightarrow 300$ K). Later it was annealed at 2500 K. This procedure was supposed to allow proper atomic redistribution during and after resolidification. This is actually a very rough method to generate a computational amorphous sample, particularly because no volume variation was allowed. Therefore, the aperiodic material thereby obtained is not expected to reproduce reliably all properties of *real* amorphous SiC. However, this simple way of operating was considered sufficient for the purpose of evaluating preliminarily the possible aspect of the topological features such as pair correlation, bondangle and bond-length distribution functions, as well as the coordination number, in an aperiodic SiC network. The topology of the reference amorphous sample is discussed in detail elsewhere [94].

For the damage-accumulation simulation, the box was divided into two zones, as shown in Fig. 2. The outer shell (1216 atoms) was used for temperature control. The recoils were introduced only in the core of the box (512 atoms) and great care was taken to avoid the production of damage in the outer shell: all simulations in which the displacement cascades were not entirely contained in the box-core were rejected and repeated. The 100-eV primary knock-on atoms (PKAs) were introduced three by three, alternating groups of Si and C atoms. Both the ballistic and the thermal spike phases of each 'triple cascade' were abundantly completed within 4000 timesteps (≈4 ps), that is, after that amount of time the temperature of the system was 20 K again. Thereafter, a 10 000-timestep (10 ps) relaxation followed, at the end of which the cohesive energy of the system was sampled and the defects were counted. The criteria adopted for counting the defects were as follows: (1) an atom was counted as *displaced* whenever it was found at a distance greater than the 1st neighbour distance ($d_1 = \sqrt{3}/4a_0$) from its original position; (2) a *replacement* occurred whenever a displaced atom was found at a distance smaller than $d_1/2$ from a *vacancy* left by another displaced atom: if the vacancy corresponded to an equilibrium position for the type of atom displaced, then a *recombination* had taken place; if, on the contrary, the vacancy was of the opposite type, then an *antisite* had formed; (3) Any displaced atom found at a distance greater than $d_1/2$ from all vacancies was counted as an *interstitial* atom. The number of interstitials, that equals the number of vacancies, is referred to as the number of *Frenkel pairs*. Concomitant with the number of defects, the dose level was calculated in terms of displacements per atom (dpa), by dividing by 512 the total number of atomic displacements accumulated up to the snapshot considered, also compared with the previous snapshot (in this case, if the same atom was displaced twice, it was counted as two displacements). Every 12th PKA, the topological distribution functions were sampled, by averaging over a 40 000-timestep run. It was necessary to accumulate 120 recoil atoms in order to amorphize the material, equivalent to 23.4 eV/atom and to 0.94 dpa. Globally, the irradiation covered a time-span of 1 ns, so that the simulated dose-rate was of the order of 10^9 dpa/s.

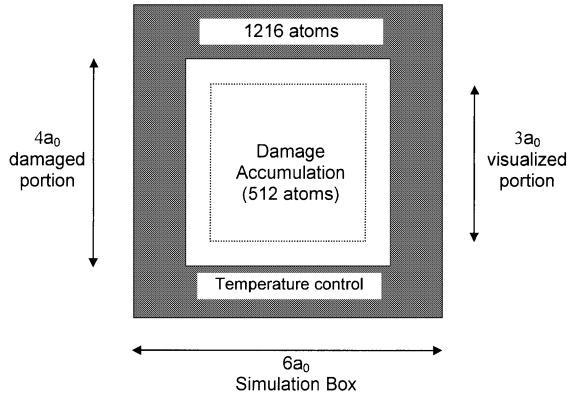

Fig. 2. Simulation box subdivision into two zones: the outer shell (1216 atoms) was used for temperature control; the recoils were introduced only in the core (512 atoms).

To anneal the irradiation-amorphized sample a two-step (20 → 1320 K, 1320 → 2320 K) 1-ns heating was performed, after which the computational material was kept at constant temperature (2320 K) for 25 ns. For the first 10 ns, every 0.5 ns (5×10^5 timesteps) the system was quenched, in order to count the defects without any thermal-agitation interference. From 10 ns onward this operation was carried out only every 5 ns (5×10^6 timesteps). Moreover, every 5 ns, after the quenching, the topological functions were sampled by averaging over a 40 000-timestep run. Quite the same procedure was utilised to anneal the reference amorphous sample. However, whereas in the *irradiation-amorphized* SiC a significant recovery was observed during annealing, in the *thermally amorphized* SiC used as a reference no substantial topological change could be detected after 20 ns at high temperature. Hence, the simulation in this second case was interrupted after that amount of time.

4. Results

4.1. Amorphization

In Fig. 3 the variation of the cohesive energy (eV/atom) in the 512-atom irradiated SiC sample is plotted against dpa. In the same figure the cohesive energies of crystalline and reference amorphous SiC are indicated (respectively, 6.41 and 5.75 eV/atom). It can be seen that, already around 0.3 dpa, the cohesive energy approaches closely the value of the amorphous system. Above 0.8 dpa it can be said that, from the cohesive energy point of view, the material has undergone a c-a transition. In Fig. 4 the evolution of the *relative* short-range order (SRO) parameter, $S_{\mathrm{SRO,r}}$, versus dpa is shown. For the SRO parameter the definition proposed by Gehlen and Cohen [96] was adopted, but the number obtained from the definition was normalised so that '1' corresponds to total order. Moreover, the magnitude plotted, $S_{\mathrm{SRO,r}}$, was referred to the level of order encountered in the reference amorphous material, $S^{\mathrm{a}}_{\mathrm{SRO}} = 0.488$, according to the transformation: $S_{\mathrm{SRO,r}} = (S_{\mathrm{SRO}} - S^{\mathrm{a}}_{\mathrm{SRO}})/(1 - S^{\mathrm{a}}_{\mathrm{SRO}})$. In this way it was possible to interpolate the data points by a simple exponential function which, however, could not account for the double slope-change between ≈0.4 and ≈0.6 dpa. Both figures (3 and 4) prove that an amorphous state was reached after accumulating 0.94 dpa. This fact is confirmed by the analysis of the topology, well synthesised in Fig. 5, where the total pair-correlation functions for the irradiated and the reference amorphous sample are compared. The shape of both distributions is typical of systems with no periodicity and the resemblance between the two curves is almost surprising, considering

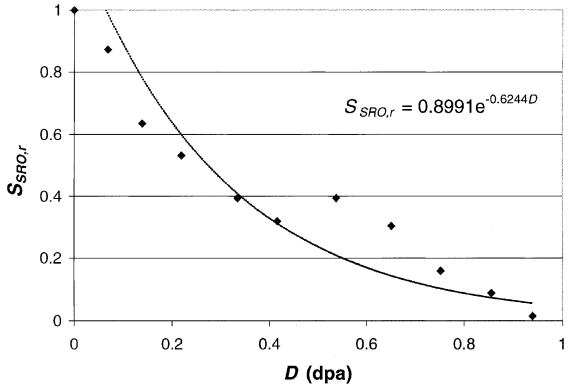

Fig. 4. Evolution of the *relative* short-range order parameter, $S_{\mathrm{SRO,r}}$ in the irradiated-SiC computational sample, versus dpa. Note the double slope-change between ≈0.4 and ≈0.6 dpa. The data points are interpolated by a simple exponential function.

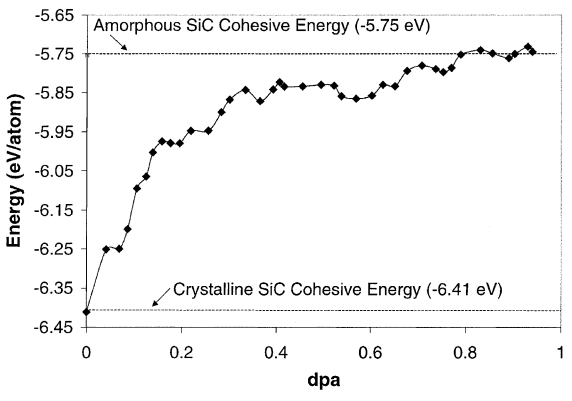

Fig. 3. Cohesive energy (eV/atom) in the 512-atom irradiated-SiC computational sample, as a function of accumulated dose (dpa).

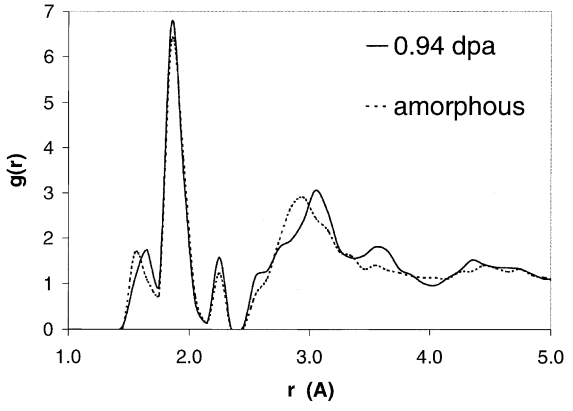

Fig. 5. Comparison of the total pair correlation function for the irradiated and the reference amorphous SiC sample. In both cases the periodicity has been lost.

the completely different simulation procedures followed in either case (see also Fig. 13(b)).

Before commenting further on the topology of the irradiation-amorphized material, as compared to the reference amorphous sample, it is convenient to illustrate the evolution with increasing dose of the number of defects, as shown in Fig. 6. It can be seen that the number of Frenkel pairs visibly grows, particularly up to ≈0.3 dpa, but goes through continuous oscillations. Also the number of recombinations evidently oscillates. This can be interpreted as a consequence of an ongoing 'struggle' between recovery and damage accumulation, which turns particularly 'harsh' in the range between ≈0.3 and ≈0.6 dpa, that is, in the same interval where the double slope-change in the SRO parameter takes place (Fig. 4). Such a double slope-change could mean that the CDC for amorphization has been reached locally, in a few points of the sample. Around 0.6 dpa the number of recombinations starts decreasing, replaced by a rise in antisite population, whereas the number of Frenkel pairs displays a tendency to saturation. Finally, in Fig. 7 the Bragg–Williams long-range order (LRO) parameter [97] diminution against dpa is shown: it should be noted that the loss of long-range order is not as spectacular as in intermetallics (0.3 [61]), a level of order as high as 0.9 being still maintained just before the c-a transition. This high value coincides with the electron-diffraction LRO estimate made by Inui et al. after irradiating SiC with 2-MeV electrons up to the critical dose for amorphization [37,39].

In Fig. 8 the bondlength and bondangle distribution functions for the irradiated and the reference amorphous SiC are compared. Though, as mentioned, both samples share the same degree of disorder and show no periodicity (Figs. 4 and 5), the profound difference between the two cases is now visible. The reference amorphous material is characterised by a slightly lower

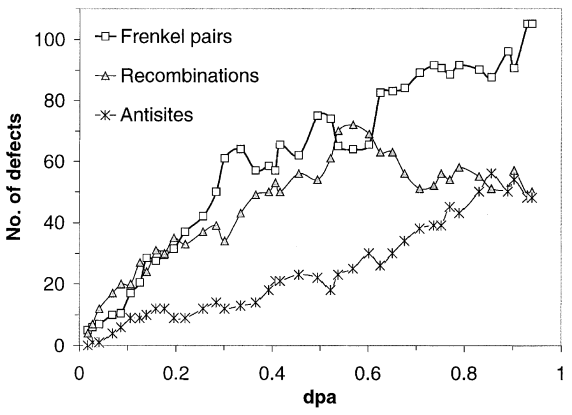

Fig. 6. Evolution with increasing dose of the number of defects in the irradiated-SiC computational sample (512 atoms).

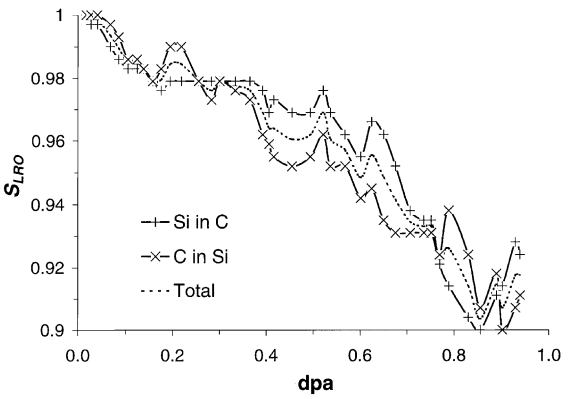

Fig. 7. Bragg–Williams long-range order parameter diminution against dpa in the irradiated-SiC computational sample. Note that at the c-a transition its value is still as high as 0.9.

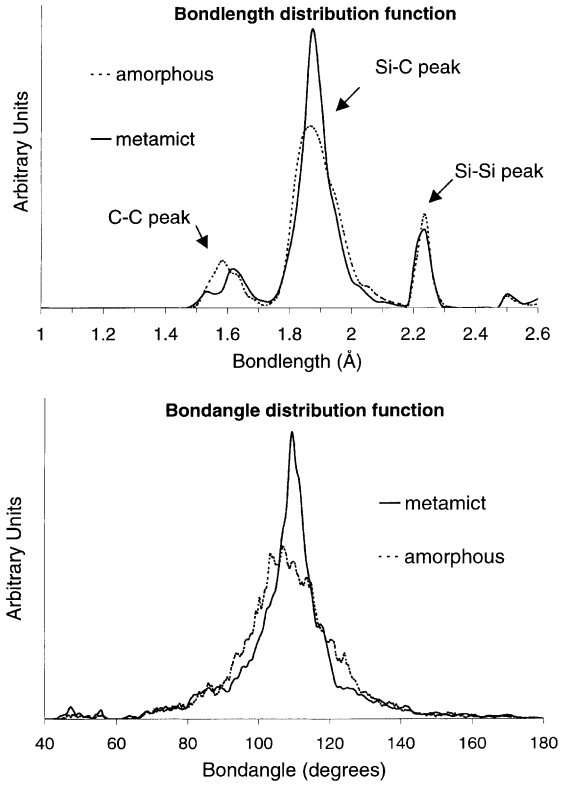

Fig. 8. Comparison between bondlength (above) and bondangle (below) distribution functions for the irradiated and the reference amorphous SiC.

percentage of heteronuclear bonds (lower SiC peak in the bondlength distribution), reflected also in the slightly lower partial coordination numbers in Table 1. More

Table 1
Total and partial coordination numbers in crystalline, reference amorphous, irradiation-amorphized and disordered SiC according to MD simulation

Coordination No.	Crystalline	Amorphous	Irradiation-Amorphized	Disordered
n	4.00	4.09	4.03	4.00
n_{Si}	4.00	4.16	4.11	4.00
n_{SiC}	4.00	2.92	3.02	3.30
n_{SiSi}	0.00	1.24	1.09	0.70
n_{C}	4.00	4.02	3.94	4.00
n_{CSi}	4.00	3.00	3.10	3.27
n_{CC}	0.00	1.02	0.84	0.73

importantly, the irradiation-amorphized state exhibits a net preference for the tetrahedral bondangle (≈109°), absent in the other sample. These differences can be compared with the experimental findings by Bolse et al. [48,49], who observed, by extended X-ray absorption fine structure (EXAFS), larger angle distortion and larger amount of homonuclear bonds in SiC irradiated much above the critical dose for amorphization, as opposed to only critically irradiated SiC. It could be speculated that the reference amorphous sample, obtained computationally by thermal treatment, may be roughly representative of the microstructure of amorphous SiC obtained by supercritical irradiation. On the contrary, the irradiation-amorphized sample, obtained by simulating the irradiation, would reflect better the topology of SiC irradiated only up to the critical level.

4.2. Annealing

In Figs. 9 and 10 the evolution against annealing time of cohesive energy and SRO parameter for the irradiation-amorphized SiC is shown. The shaded area corresponds to the heating phase. It can be seen that a prompt recovery takes place: both magnitudes reach, in about 8–9 ns, an asymptotical (in the time-span covered) value, corresponding to a final state which is *intermediate* between the amorphous and the crystal ($S_{SRO} < 1$). In order to understand what characterises such an intermediate state it is useful to examine the evolution of the number of defects, as given in Fig. 11. About 80% of the Frenkel pairs disappear in a matter of ≈7 ns: most of them annihilate, but a substantial fraction (≈40%) recombines 'wrongly', thereby creating a considerable amount of antisites. This is reflected by the variation of the LRO parameter, which keeps decreasing during the annealing, contrary to the SRO parameter (Fig. 12). An inspection of the topological functions [94] (not shown in this paper) reveals that the effect of the annealing was the production of disordered SiC, i.e. a system with structural periodicity, but rich in antisites. This can be seen more clearly in Table 1, where the coordination numbers for the crystalline, reference amorphous, irradiation-amorphized and disordered samples are listed according to simulation. In the last case all atoms are four-coordinated, as in the perfect crystal, but often one neighbour is of the same type (see also Fig. 13(c)). By the way, this observation suggests that the remaining

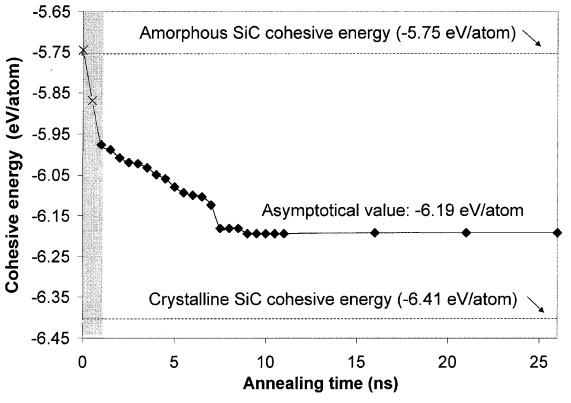

Fig. 9. Cohesive energy evolution against annealing time for the irradiation-amorphized SiC sample. The shaded area corresponds to the heating phase, as described in Section 3.

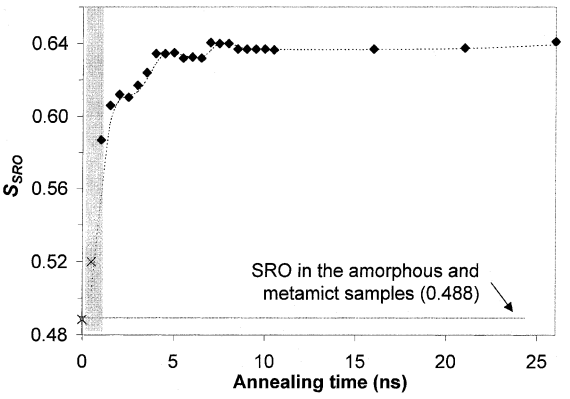

Fig. 10. Short-range order parameter evolution against annealing time for the irradiation-amorphized SiC sample. The shaded area corresponds to the heating phase, as described in Section 3.

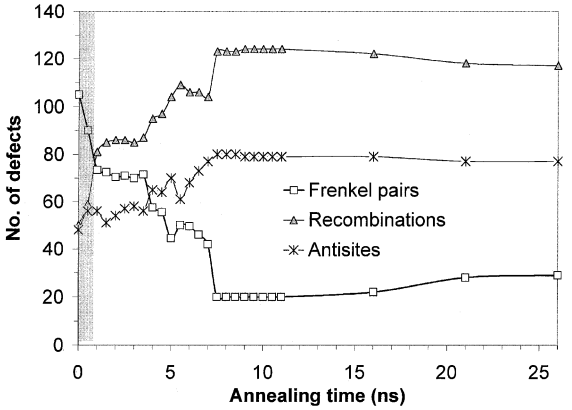

Fig. 11. Defect number evolution against annealing time for the irradiation-amorphized SiC sample. The shaded area corresponds to the heating phase, as described in Section 3.

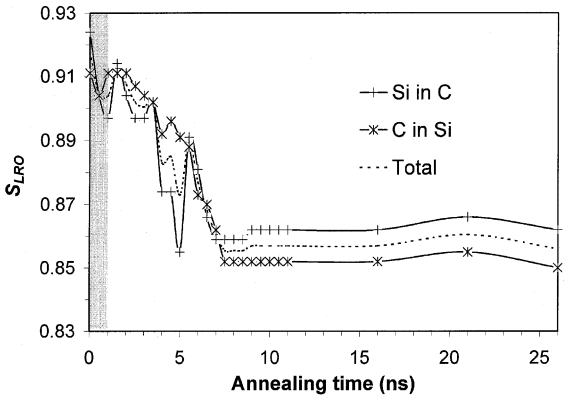

Fig. 12. Long-range order parameter evolution against annealing time for the irradiation-amorphized SiC sample. The shaded area corresponds to the heating phase, as described in Section 3.

interstitials in the disordered SiC sample prefer tetrahedral (4-coordinated) locations. The meaning of the slight increase in the number of Frenkel pairs in Fig. 11 after 15 ns (to the detriment of replacements) is not clear but it should not be considered a real long-term trend (though in order to be sure of it, the annealing should have been protracted for much longer times). It seems likely, instead, that it consists of an effect of the very high simulation temperature. In a disordered network, particularly in the vicinities of a defect, the mere thermal agitation can be the cause of a temporary, or apparent, atomic displacement. It should be borne in mind that a replacing atom will be recognised by the code as an interstitial when it is only 0.95 Å away from the vacancy previously occupied.

Contrary to the irradiation-amorphized material, after annealing for 20 ns the reference amorphous

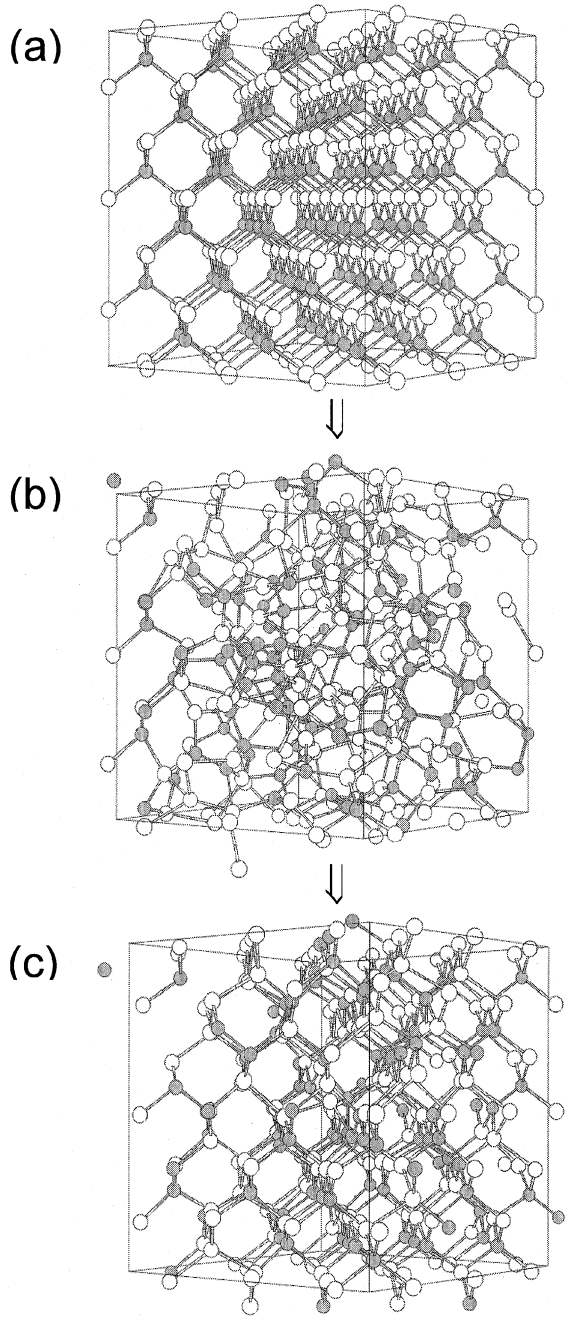

Fig. 13. 'Stick-and-ball' visualization of the three states of the computational SiC sample: (a) perfect crystal, (b) irradiation-amorphized and (c) disordered. Grey balls are C atoms, white balls are Si atoms.

sample no sign of recovery was observed: the aperiodic (lack of) structure was strictly maintained, except for a slight tendency to diminution in the number of homonuclear bonds and a feebly higher peak around 109° in the bondangle distribution [94] (no relevant figures are

shown in this paper). Again, this might perhaps suggest a certain resemblance with supercritically amorphized SiC, whose recovery has been seen experimentally to be more difficult than for samples irradiated only up to the critical dose [10,12,15,16,35].

5. Discussion of the simulation

5.1. Simulation and experiment

The major shortcoming of the simulation is the unrealistically high dose-rate (10^9 dpa/s). On the other hand, it seems reasonable to assume that dose-rate effects should only be measurable when diffusion mechanisms can compete with defect production. This competition should not exist at all at cryogenic temperature. It was also for this reason that the simulation was conducted at 20 K: it allows one to compare the relevant results with low-temperature experimental observations, virtually insensitive to dose-rate effects. For example, the average critical energy density for amorphization measured experimentally at 77 K is around $\approx$20 eV/atom [51] and this value agrees with the 23.4 eV/atom found in the simulation. Less certain is the legitimacy of comparing the MD-calculated critical dpa level with the corresponding experimentally deduced value, normally obtained by using either the TRIM/SRIM-code displacement data, in the case of ion irradiation [21–25,28–30,50,52–54], or adequate conversion tables, in the case of electron irradiation [28,52,98]. At any rate, the simulated value of 0.94 dpa compares well with $\approx$1 dpa calculated both by Weber, on the basis of Inui's experimental electron-irradiation results [37,39,52], and by Zinkle and Snead, on the basis of Matsunaga's [38,47]. This seems consistent with the fact that the 100 eV cascades simulated are representative of the average PKA energy spectrum under 2 MeV-electron bombardment. Furthermore, we already mentioned the coincidence between simulated and measured LRO parameter, at the threshold for the c-a transformation (0.9). Globally, it can be concluded that the simulation has been able to reproduce correctly the values of the main experimental magnitudes governing the irradiation-induced c-a transition.

5.2. Mechanisms of amorphization

To discuss the microscopic mechanisms leading to low-temperature amorphization it is useful to refer to Figs. 4 and 6. As already suggested, the competition between recombinations and Frenkel pairs becomes critical between $\approx$0.3 and $\approx$0.6 dpa. After that point the number of Frenkel pairs saturates and recombinations start diminishing, whereas antisites grow. This fact might lead one to believe that the retarded contribution of disorder onset (antisites) is crucial to the occurrence of the phase-change. However, it should be noted that, after accumulating 0.6 dpa, the network is already so distorted, that it is hard to define what an antisite is. The code can spot such defects because it compares the coordinates of the current atomic locations with those of their original sites in the perfect lattice, by applying the criteria stated in Section 3. But it is quite clear that the increase in the number of antisites detected during the last stage of the irradiation should more realistically be ascribed to the complete revolution of atomic positions induced by the amassment of Frenkel pairs, than to simple exchanges of atomic positions, as it appears obvious after looking at Fig. 13(b). Moreover, however high the number of antisites can get, they always represent a minority and, by comparing Figs. 3 and 6, it is patent that the major energy change in the material takes place due to the growth of the Frenkel-pair number, the final antisite increase scarcely influencing the energetics of the system. On the other hand, during the annealing the number of antisites increases visibly, but still the sample does not turn amorphous; in fact, it regains its periodicity, as is manifest in Fig. 13(c). In summary, all signs indicate that the accumulation of Frenkel pairs is the main responsible for the creation of an aperiodic and highly distorted network in the material, recognisable as amorphous, the role of antisites in the process being negligible.

From the theoretical point of view, it has been demonstrated by Pedraza [65,66] that Frenkel pairs are perfectly capable of causing irradiation-induced amorphization, as long as a mechanism can be identified that allows the coexistence of vacancies and interstitials, by impeding their annihilation. In the case of intermetallics, Pedraza had to list a series of conditions that these interstitial/vacancy (I/V) complexes should satisfy, to justify their survival. However, in the case of SiC things are much simpler, as MD simulations have clearly revealed the existence, in this material, of energy barriers that prevent recombination even when the interstitial lies very close to a free vacancy [69–72]. In particular, it has been demonstrated that the lifetime τ of these I/V complexes depends on temperature T according to an Arrhenius law [72]

$$\tau = \frac{1}{\nu_D} \exp\left(\frac{E_b}{k_B T}\right), \tag{3}$$

where ν_D is the Debye frequency ($\approx 2.5 \times 10^{13}$ Hz, obtained by interpolating simulated lifetime points and in good agreement with the experimental value), k_B the Boltzmann constant and E_b is the energy barrier. This energy was calculated for a particular case and a value of 1.16 eV was found [72]. The temperature dependence expressed by (3) might explain the existence of a critical temperature for amorphization, as the analytical model

presented in the next section will show. Finally, it is useful to mention that an estimate of the recombination distance obtained dividing the volume of the 512-atom simulation box by the number of Frenkel pairs at the saturation (≈100) yields $0.53a_0$, which is a perfectly acceptable value for a covalent material [99].

5.3. Mechanisms of recovery

Where antisites do play a role is during the recovery of the material. It has been seen that the effect of the annealing is helping the material regain its periodicity, though retaining chemical disorder. In fact, the disorder increases and the sample ends up in a situation *intermediate* between amorphous and crystalline. Clearly, recovering from this intermediate state implies reordering, whose occurrence is likely to be linked with the onset of vacancy migration, that is an especially slow process, activated only at high enough temperatures [74]. Hence, it can be said that the formation of antisites hampers the complete recovery of the material.

It was possible to find several experimental results supporting the qualitative picture offered by the simulation, or interpretable on its basis. Many of the experimental results that will be mentioned (or have been mentioned) were obtained by irradiating SiC with ions or neutrons. It is true that these particles produce recoils of much higher energy than the 100 eV here simulated and that, in principle, different states of damage could thereby be produced. However, MD simulations of displacement cascades in SiC induced by self-ions of up to 8 keV have shown that the number of defects per cascade grows linearly with the energy of the recoils [95]. Therefore, the proportion of antisites/Frenkel pairs per cascade, that is the key parameter to decide which sort of defects the destabilization into the amorphous state should be ascribed to, is independent of the recoil-energy up to significantly high recoil-energy values. The same MD simulations revealed that hardly any large cluster is produced in a self-ion displacement cascade in SiC [94], the only exception to this behaviour being obtained by considering very-high-mass impinging ions [68]. Finally, even after overlapping up to 25 high-energy (3 keV) cascades, as long as the accumulated dose is much lower than the critical dose for amorphization, the number of defects increases linearly with the number of cascades [69]. For all these reasons, it does not seem preposterous to extend the validity of the results of the low-energy self-recoil simulation herein presented to the case of ion or neutron irradiation. Only the case of very-high-mass impinging particles should be definitely excluded. The only aspect that should change, when irradiating with higher-energy recoils, is that a lower number of impinging particles is enough to reach the Frenkel pair critical concentration, as is indeed observed experimentally (the critical dose for amorphization is lower when irradiating with ions). This stated, it is possible to turn to the experimental evidence supporting the results of the simulation.

Nikolaenko et al. measured, by X-ray diffraction, the degree of disorder produced in SiC by neutron-irradiation (3.2×10^{21} n/cm^2, $E > 75$ eV). They observed a *further decrease* in the LRO parameter by annealing, at 250°C, a sample which had been irradiated at 90°C. The degree of order was observed to *recover* only after 1 h at 450°C [100]. Musumeci et al., after ion-irradiating SiC samples up to the critical dose for amorphization, or just below it, monitored the evolution of optical properties such as transmittance when the beam was turned off, at room temperature. They could witness a rapid recovery, but only up to a transmittance value which was *intermediate* between crystal and amorphous [34]. Jiang and Weber, who measured by RBS-C the damaged fraction in low-temperature C^+-implanted, and subsequently high-temperature annealed, SiC samples, plotted curves very similar to Musumeci's, observing quicker recovery as the annealing temperature was raised, down to a state *intermediate* between amorphous and crystalline [23]. Finally, in an old neutron-irradiation work, Thorne et al. realised that the change in irradiated-SiC thermal diffusivity (1.8×10^{21} n/cm^2) saturates faster than swelling and attributed this fact to the existence of defects that, without causing expansion, could have an influence on heat transfer properties [101]. Antisites satisfy this condition. They also observed that, upon annealing, irradiated-SiC thermal diffusivity recovered at higher temperature than swelling [101]. The production of a higher number of antisites during annealing as a way to eliminate swelling, together with their role as a bottleneck for the recovery process, can well explain this experimental observation.

6. Analytical model

The basic ideas behind the model that is going to be presented are as follows: (1) the irradiation-induced amorphization of SiC is achieved as soon as a CDC is reached, the defects to be considered being Frenkel pairs; (2) no DIA takes place; (3) a substantial fraction ε of the Frenkel pairs generated by irradiation at low temperature are metastable and their lifetime is expressed by the Arrhenius law (3). The fundamental magnitude to be calculated is the concentration of Frenkel pairs, c_{FP}, whose critical value, $c_{\mathrm{FP,c}}$, estimated according to the simulation, is ≈20% (≈1.9×10^{22} cm^{-3}). It will be assumed that the time variation of c_{FP} is described by the following, simple rate equation:

$$\frac{\mathrm{d}c_{\mathrm{FP}}}{\mathrm{d}t} = n_{\mathrm{FP}}\Phi - \varepsilon\frac{c_{\mathrm{FP}}}{\tau} - \sigma_0\Phi c_{\mathrm{FP}}, \tag{4}$$

where n_{FP} is the number of Frenkel pairs produced by an incident particle per unit length, Φ the radiation flux, ε the fraction of metastable Frenkel pairs, τ their lifetime, given by relation (3), and σ_0 is a radiation-induced reordering cross-section. According to this approach, a temperature-decreasing equilibrium concentration $c_{FP,eq}$ will be reached after a transient. Depending on whether this equilibrium concentration is higher or lower than $c_{FP,c}$, the c-a transition will occur or will not. The critical temperature for amorphization can therefore be calculated by equalling $c_{FP,eq}$ and $c_{FP,c}$, thereby obtaining

$$T_c = \frac{E_b/k_B}{\ln((1/D_\Phi)/(1/D_0 - \sigma_0))}, \tag{5}$$

where $D_\Phi = \Phi/\varepsilon\nu_D$ and $D_0 = c_{FP,c}/n_{FP}$ have the dimension of a dose (cm^{-2}). The exponential solution $c_{FP}(t)$ to Eq. (4) is easily obtained by imposing the initial condition $c_{FP}(0) = 0$. Assuming that $T < T_c$, by equalling the solution $c_{FP}(t)$ to $c_{FP,c}$ a temperature-dependent critical time t_c is found, when the CDC is reached. The product Φt_c then yields the critical dose for amorphization, D_c, as a function of temperature

$$D_c(T) = \frac{1}{1/D_\Phi \exp(-E_b/k_BT) + \sigma_0} \times \ln\frac{1}{1 - D_0(1/D_\Phi \exp(-E_b/k_BT) + \sigma_0)}. \tag{6}$$

This equation is consistent with the general theoretical framework provided by Weber in a recent paper [102]. The most interesting feature of this expression is that its limit for $T \to 0$ and $\sigma_0 \to 0$ is D_0, that is, it generates naturally a value for the 0-K critical dose for amorphization, whose expression, $D_0 = c_{FP,c}/n_{FP}$, closely resembles the critical energy density model by Dennis and Hale [60]. Moreover, it predicts a vertical asymptote in correspondence with T_c and the physical meaning of E_b is clear: it is the average height of the energy barrier that an interstitial has to overcome, by thermal agitation, in order to occupy a vacancy. The value of this energy is expected to be higher than the 1.16 eV mentioned earlier, as it includes the formation of antisites. Note that the role of σ_0 is simply stabilising numerically the formula for $T \to 0$, so that, for practical purposes, any small value assigned to this parameter, for example 10^{-24} cm^2, will do.

By displacement-cascade MD simulation it was estimated that $n_{FP} \approx 7 \times 10^7$ cm^{-1} [94,95], so that $D_0 \approx 2.7 \times 10^{14}$ cm^{-2} or, turning to dpa (taking a number of atomic displacements per unit length $n_D \approx 11 \times 10^7$ cm^{-1} [94,95], $D_0 \approx 0.3$ dpa. This is a typical value for the critical ion-dose for amorphization at cryogenic temperature. The estimate of the critical temperature using (5), on the other hand, is very sensitive to the choice of E_b. With a flux the order of $\approx 10^{12}$ cm^{-2} s^{-1} and choosing, on the basis of the results of the simulation, $\varepsilon \approx 0.8$, T_c is found to vary between $\approx$380 K ($E_b = 1.2$) and $\approx$500 K ($E_b = 1.5$), in agreement with the typical range of variations of T_c, 300–500 K [21,28,36–39,42,50–54]. Therefore, the model seems promising. Nonetheless, however good the agreement of the calculated D_0 and T_c with the experimental values, using expression (6) alone it is impossible to interpolate correctly the experimental data points provided by Weber for the function $D_c(T)$, as measured by in situ transmission electron microscopy (TEM) after bombarding β-SiC with 1.5-MeV Xe^+ ions [28]. A probable reason for this is that the energy barrier mechanism, deduced from the MD simulation, is possibly not the only one competing with irradiation-induced amorphization. In particular, one mechanism that the MD simulation could not take into account is interstitial migration. The following, *totally intuitive* assumptions were then made: (1) expression (6) only represents the contribution to D_c of the fraction ε of metastable, or short-lived, Frenkel pairs; (2) the contribution of interstitial migration can be taken into account, within a *supposedly* linear approximation, by simply adding to (6) the expression (2), referred only to the fraction $(1 - \varepsilon)$ of *stable* Frenkel pairs. In other words, it was admitted that the experimental data points could be interpolated correctly using the *compound* expression:

$$D_c(T) = \frac{1}{1/D_\Phi \exp(-E_b/k_BT) + \sigma_0} \times \ln\frac{1}{1 - D_0(1/D_\Phi \exp(-E_b/k_BT) + \sigma_0)} + (1 - \varepsilon)\frac{A}{\sqrt{\Phi_{dpa}}} \exp\left(-\frac{E_m^i}{2k_BT}\right), \tag{7}$$

where the flux in the second addend is expressed in dpa/s, in order to preserve the consistency with the numbers used by Snead and Zinkle for their interpolation [50]. Clearly, this approach is far from being mathematically rigorous. Yet, it proves useful, as using (7) the data by Weber [28] can be interpolated with excellent approximation, as shown in Fig. 14, where the curve obtained from expression (6) alone is also plotted and the 'best-fit' parameters are indicated. Note in particular that the best-fit value for the energy barrier was found to be $E_b = 1.53$ eV, the interstitial migration energy value being the same as in [50], i.e. 0.56 eV.

Weber's expression (1) is functionally much simpler than (7) and works in general quite well. Still, expression (7) contains an explicit reference to two clear microscopic mechanisms, each of them responsible for one effect. As it is, the 'boundaries' of the $D_c(T)$ function (D_0 and T_c) are determined by the accumulation at low temperature and quick disappearance at high enough temperature of the metastable Frenkel pairs, whose lifetime depends on temperature according to the Arrhenius law (3). On the other hand, the gradual

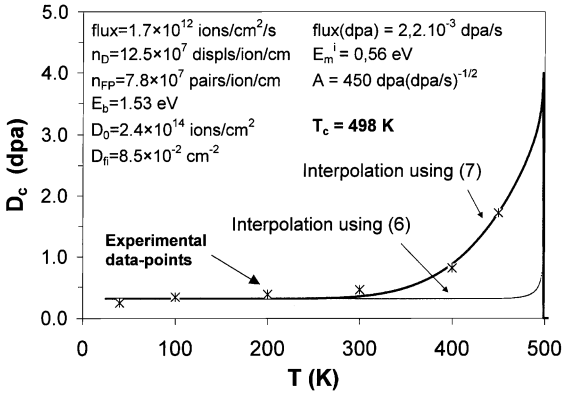

Fig. 14. Interpolation of the experimental data points by Weber [28] (in situ TEM after bombarding β-SiC with 1.5-MeV Xe^+ ions) with a curve obtained from the intuitive, *compound* expression (7). The curve corresponding to expression (6) alone is also plotted. All 'best-fit' parameters are indicated.

growth of D_c in the intermediate temperature range, below T_c, is accounted for by interstitial migration, possibly – as suggested by Weber [102] – assisted by radiation. However, the latter mechanism alone, without the disappearance of metastable Frenkel pairs, would not explain the existence of such a 'sharp edge' in correspondence with the critical temperature, at least according to Motta and Olander's model [50,67].

In summary it can be said that the model herein hinted at, partly stemming from the results of the MD simulation and partly from past theoretical models, though extremely rough and definitely oversimplified, outlines the necessity of at least two microscopic mechanisms, opposing the irradiation-induced amorphization of SiC, to predict the shape of the $D_c(T)$ curve: (1) quick recombination, in a restricted temperature range, of metastable Frenkel pairs and (2) interstitial migration. Supposedly, a rigorous mathematical treatment that includes both of these 'ingredients' in the source differential equations should lead to a more accurate model, capable of reproducing correctly most experimental results.

7. Conclusions

- The MD simulation of SiC irradiation-induced amorphization by accumulation of radiation damage up to a critical defect concentration, followed by partial annealing, not only reproduced correctly the values of experimentally measured magnitudes, but also provided a satisfactory explanation for several experimental observations, from the microscopic standpoint.
- The accumulation of Frenkel pairs at low temperature, up to a concentration on the order of 1.9×10^{22} pairs/cm^3, made possible by the existence of recombination barriers, seems to be the microscopic mechanism responsible for SiC irradiation-induced lattice distortion and destabilisation, leading to the c-a transition.
- Antisites do not play any significant role in determining the transition to the amorphous state induced by irradiation. However, their number increases visibly during annealing, as experimentally observed, leading to the formation of a periodic but chemically disordered network. The reordering through vacancy diffusion could be the bottleneck for complete recovery.
- It is likely that the topology of irradiation-amorphized SiC obtained by irradiating much above the critical dose is substantially different from the topology of only critically irradiated SiC, the former being characterised by a higher fraction of homonuclear bonds and higher bondangle distortion. This difference, observed experimentally and speculatively suggested by the simulation, might be partly responsible for the more difficult recovery of supercritically irradiated SiC.
- The elaboration of a simple analytical model, mainly based on the results of the simulation, has shown that the Arrhenius-type law predicting the lifetime of metastable Frenkel pairs formed at low temperature after irradiation can explain the existence of a critical temperature for amorphization, above which irradiation-induced amorphization turns impossible, however high the dose. As it is, above this temperature it ceases to be feasible to accumulate Frenkel pairs up to the required concentration.
- To interpolate correctly the experimental data points describing the increase of the critical dose for amorphization with temperature (below the critical temperature for amorphization), it is necessary to take into account also the effect of interstitial migration, as a mechanism opposed to the accumulation of damage in the material.

Acknowledgements

The authors wish to acknowledge the contributions of Tomás Díaz de la Rubia (LLNL, USA), Luciano Colombo (University of Cagliari, Italy) and Bill Weber (PNL, USA) to the accomplishment of this work. Work financed by the EU-Commission: Marie Curie Research Training-Grant, Fusion Programme, Contract no. ERB-5004-CT97-5002.

References

[1] L.H. Rovner, G.R. Hopkins, Nucl. Technol. 29 (1976) 274.
[2] S. Sharafat, F. Najmabadi, C.P.C. Wong, Fus. Eng. Des. 18 (1991) 215.

[3] A.S. Pérez, Ramírez et al., J. Nucl. Mater. 233–237 (1996) 1257.
[4] S. Ueda et al., DREAM Design Team, J. Nucl. Mater. 258–263 (1998) 1589.
[5] McDonnell-Douglas Aerospace Team, DOE/ER-54101 MDC92E0008, vols. I, II and III, March 1992.
[6] B. Badger et al., Kernforschungszentrum Karlsruhe Report no. KfK-3202/Madison, University of Wisconsin Fusion Technology Institute Report no. UWFDM-450, June 1981.
[7] J.M. Perlado et al., J. Nucl. Mater. 233–237 (1996) 1523.
[8] G.R. Hopkins, J. Chin, J. Nucl. Mater. 141–143 (1986) 148.
[9] R.B. Wright, D.M. Gruen, Rad. Eff. 33 (1977) 133.
[10] A. Pérez-Rodríguez et al., J. Electr. Mater. 25 (1996) 541.
[11] R.R. Hart, H.L. Dunlap, O.J. Marsh, Rad. Eff. 9 (1971) 261.
[12] J.M. Williams, C.J. McHargue, B.R. Appleton, Nucl. Instrum. and Meth. 209/210 (1983) 317.
[13] J.A. Spitznagel et al., Nucl. Instrum. and Meth. B 16 (1986) 237.
[14] H.G. Bohn et al., J. Mater. Res. 2 (1987) 107.
[15] A. Föhl, R.M. Emrick, H.D. Carstanjen, Nucl. Instrum. and Meth. B 65 (1992) 335.
[16] N.G. Chechenin et al., Nucl. Instrum. and Meth. B 65 (1992) 341.
[17] A. Heft et al., Mater. Sci. Eng. B 29 (1995) 142.
[18] L.L. Snead, S.J. Zinkle, Mater. Res. Soc. Symp. Proc. 373 (1995) 377.
[19] W.J. Weber, L.M. Wang, N. Yu, Nucl. Instrum. and Meth. B 116 (1996) 322.
[20] M.G. Grimaldi et al., J. Appl. Phys. 81 (1997) 7181.
[21] W.J. Weber et al., J. Nucl. Mater. 244 (1997) 258.
[22] W. Jiang et al., Nucl. Instrum. and Meth. B 143 (1998) 333.
[23] W. Jiang et al., Nucl. Instrum. and Meth. B 148 (1998) 562.
[24] W. Jiang, W.J. Weber, S. Thevuthasan, Mat. Res. Soc. Symp. Proc. 540 (1999) 183.
[25] L.L. Snead et al., Mat. Res. Soc. Symp. Proc. 540 (1999) 165.
[26] K. Kawatsura et al., J. Nucl. Mater. 271–272 (1999) 11.
[27] J.A. Edmond et al., J. Mater. Res. 3 (1988) 321.
[28] W.J. Weber, L.M. Wang, Nucl. Instrum. and Meth. B 106 (1995) 298.
[29] W.J. Weber, N. Yu, Mater. Sci. Forum 239–241 (1997) 155.
[30] W.J. Weber, N. Yu, L.M. Wang, J. Nucl. Mater. 253 (1998) 53.
[31] E. Wendler et al., Nucl. Instrum. and Meth. B 116 (1996) 398.
[32] P. Musumeci et al., Nucl. Instrum. and Meth. B 116 (1996) 327.
[33] P. Musumeci et al., Appl. Phys. Lett. 69 (1996) 468.
[34] P. Musumeci et al., Nucl. Instrum. and Meth. B 127/128 (1997) 360.
[35] E. Wendler et al., Nucl. Instrum. and Meth. B 127/128 (1997) 341.
[36] H. Inui, H. Mori, H. Fujita, Acta Metall. 37 (1989) 1337.
[37] H. Inui, H. Mori, H. Fujita, Philos. Mag. B 61 (1990) 107.
[38] A. Matsunaga et al., J. Nucl. Mater. 179–181 (1991) 457.
[39] H. Inui et al., Philos. Mag. B 65 (1992) 1.
[40] H. Inui, H. Mori, T. Sakata, Philos. Mag. B 66 (1992) 737.
[41] L.L. Snead et al., Nucl. Instrum. and Meth. B 141 (1998) 123.
[42] L.L. Snead, J.C. Hay, J. Nucl. Mater. 273 (1999) 213.
[43] C.J. McHargue, C.S. Yust, J. Am. Ceram. Soc. 67 (1984) 117.
[44] C.J. McHargue et al., Nucl. Instrum. and Meth. B 16 (1986) 212.
[45] C.J. McHargue, Nucl. Instrum. and Meth. B 19/20 (1987) 797.
[46] C.J. McHargue, P.S. Sklad, C.W. White, Nucl. Instrum. and Meth. B 46 (1990) 79.
[47] S.J. Zinkle, L.L. Snead, Nucl. Instrum. and Meth. B 116 (1996) 92.
[48] W. Bolse et al., Mater. Sci. Forum 248–249 (1997) 319.
[49] W. Bolse, Nucl. Instrum. and Meth. B 141 (1998) 133.
[50] L.L. Snead, S.J. Zinkle, Mater. Res. Soc. Symp. Proc. 439 (1997) 595.
[51] E. Wendler, A. Heft, W. Wesch, Nucl. Instrum. and Meth. B 141 (1998) 105.
[52] W.J. Weber et al., Mater. Sci. Eng. A 253 (1998) 62.
[53] W. Jiang et al., Surf. Interface Anal. 27 (1999) 179.
[54] W.J. Weber et al., Mat. Res. Soc. Symp. Proc. 540 (1999) 159.
[55] J.R. Parsons, Philos. Mag. 12 (1965) 1159.
[56] F.F. Morehead Jr., B.L. Crowder, Rad. Eff. 6 (1970) 27.
[57] F.L. Vook, H.J. Stein, Rad. Eff. 2 (1969) 23.
[58] M.L. Swanson, J.R. Parsons, C.W. Hoelke, Rad. Eff. 9 (1971) 249.
[59] J.F. Gibbons, IEEE Proc. 60 (1972) 1062.
[60] J.R. Dennis, E.B. Hale, J. Appl. Phys. 49 (1978) 1119.
[61] D.E. Luzzi et al., Acta Metall. 4 (1986) 629.
[62] D.E. Luzzi, M. Meshii, Res Mechanica 21 (1987) 287.
[63] L.W. Hobbs, C.E. Jesurum, B.A. Berger, Mat. Res. Soc. Symp. Proc. 540 (1999) 717.
[64] Y. Limoge, A. Barbu, Phys. Rev. B 30 (1984) 2212.
[65] D.F. Pedraza, J. Mater. Res. 1 (1986) 425.
[66] D.F. Pedraza, L.K. Mansur, Nucl. Instrum. and Meth. B 16 (1986) 203.
[67] A.T. Motta, D.R. Olander, Acta Metall. Mater. 38 (1990) 2175.
[68] MD simulations of displacement cascades in SiC, induced by self-ions to which the mass of Au is given, seem to suggest that large clusters may be formed within the cascade, so that maybe DIA could take place in that case (W.J. Weber, F. Gao, private communication, still unpublished).
[69] J.M. Perlado, L. Malerba, T. Díaz de la Rubia, Fus. Technol. 34 (1998) 840.
[70] J.M. Perlado, L. Malerba, T. Díaz de la Rubia, Mat. Res. Soc. Symp. Proc. 540 (1999) 171.
[71] J.M. Perlado, L. Malerba, A. Sánchez-Rubio, T. Díaz de la Rubia, J. Nucl. Mater. 276 (2000) 235.
[72] L. Malerba, J.M. Perlado, A. Sánchez-Rubio, I. Pastor, L. Colombo, T. Díaz de la Rubia, Molecular dynamics simulation of defect production in irradiated β-SiC, J. Nucl. Mater. 283–287 (2000) 794.
[73] J. Bloch, J. Nucl. Mater. 6 (1962) 203.
[74] E.M. Schulson, J. Nucl. Mater. 83 (1979) 239.
[75] C.J. McHargue, J.M. Williams, Nucl. Instrum. and Meth. B 80/81 (1993) 889.
[76] D.E. Luzzi, M. Meshii, Scripta Metall. 20 (1986) 943.
[77] M.J. Caturla et al., Phys. Rev. B 54 (1996) 16683.

[78] C. Jaouen et al., J. Appl. Phys. 65 (1989) 1499.
[79] S.U. Campisano et al., Nucl. Instrum. and Meth. B 80/81 (1989) 514.
[80] N. Hecking, K.F. Heidemann, E. Te Kaat, Nucl. Instrum. and Meth. B 15 (1986) 760.
[81] T. Díaz de la Rubia, M.J. Caturla, M. Tobin, Mater. Res. Soc. Symp. Proc. 373 (1995) 555.
[82] W.J. Weber, L.M. Wang, Nucl. Instrum. and Meth. B 91 (1994) 63.
[83] T. Díaz de la Rubia, M.W. Guinan, J. Nucl. Mater. 174 (1990) 151.
[84] J. Tersoff, Phys. Rev. B 39 (1989) 5566.
[85] J. Tersoff, Phys. Rev. Lett. 64 (1990) 1757.
[86] K. Nordlund, N. Runeberg, D. Sundholm, Nucl. Instrum. and Meth. B 132 (1997) 45.
[87] R. Devanathan, T. Díaz de la Rubia, W.J. Weber, J. Nucl. Mater. 253 (1998) 47.
[88] M. Tang, S. Yip, J. Appl. Phys. 76 (1994) 2719.
[89] M. Tang, S. Yip, Phys. Rev. B 52 (1995) 15150.
[90] H. Huang et al., Modelling Simulation Mater. Sci. Eng. 3 (1995) 615.
[91] P.C. Kelires, Europhys. Lett. 14 (1991) 43.
[92] J. Tersoff, Phys. Rev. B 49 (1994) 16349.
[93] D. Mura et al., Phys. Rev. B 58 (1998) 10357.
[94] L. Malerba, Ph.D. Thesis, Universidad Politécnica de Madrid, Spain, 2000.
[95] L. Malerba, J.M. Perlado, I. Pastor, T. Díaz de la Rubia, Molecular dynamics simulation of radiation damage production in cubic silicon carbide, in: Effects of Radiation on Materials: 20th International Symposium, ASTM STP 1405, accepted (publication: 2002).
[96] P.C. Gehlen, J.B. Cohen, Phys. Rev. 139 (1965) 844.
[97] $S_{\mathrm{LRO}} = 1 - 2N_{\mathrm{BA}}/N_{\mathrm{A}}$; N_{AB} = number of antisites (B atoms in A positions), N_{A} = number of A positions.
[98] O.S. Oen, Cross-sections for atomic displacements in solids by fast electrons, ORNL-4897, August 1973.
[99] M. Sayed et al., Nucl. Instrum. and Meth. B 102 (1995) 232.
[100] V.A. Nikolaenko, V.G. Gordeyev, V.N. Kuznetsov, Rad. Eff. 27 (1976) 163.
[101] R.P. Thorne, V.C. Howard, B. Hope, Proc. Br. Ceram. Soc. 7 (1967) 449.
[102] W.J. Weber, Nucl. Instrum. and Meth. B 166–167 (2000) 98.